Robotica (2000) volume 18, pp. 13–21. Printed in the United Kingdom © 2000 Cambridge University Press

High-speed manipulation by using parallel wire-driven robots

Sadao Kawamura†, Hitoshi Kino†† and Choe Won†††

SUMMARY

A new type of a parallel wire-driven robot is proposed in order to reach ultra-high speed. The driving principle of parallel wire systems is described. Since wires can only pull and not push on an object, at least $n+1$ wires are needed in order to move the object in a n-dimensional space. In this paper, taking account of the effect of such redundancy on actuation, the motion stability in wire length coordinates is analyzed by using a Lyapunov function. Using "Vector Closure", it is proven that the hand position and orientation converge to the corresponding desired values and the internal force also converges to the desired one. Moreover, by making good use of non-linear elasticity of parallel wire driven robots, it is claimed that the internal force arising from redundant actuation can effectively reduce vibration when the high-speed robot stops at desired points. As a result, ultra-high speed with more than 40 g(g:gravitational acceleration) can be attained by using relatively small actuators.

KEYWORDS: Parallel wire-driven robot; High speed; Stability analysis; Non-linear elasticity

1. INTRODUCTION

Since robots work in place of humans in many fields, it might be natural to design a robot manipulator which has a similar serial link structure to human arms. However, if we desire to exceed human motion ability, for example, ultra-high speed, ultra-high precision and so on, it is not necessary to employ a human-like structure. A serial-link structure like human arms must support the mass of the arm itself in addition to pay load, i.e. actuator power must support and move the robot itself. Therefore, even if large actuators are utilized, it is very difficult to realize high speed motions. As a result, a very large and heavy robot is designed.[1] Furthermore, as regards the position accuracy of robots, it is well known that a serial-link structure has a disadvantage that joint angle errors are accumulated in the series.

To avoid such difficulties, a parallel link structure was proposed. In a parallel link structure, all actuators are placed on the base of the robot. Therefore, each actuator does not need to support or drive the mass of other actuators. As a result, relatively small robots whose actuators are also small can generate high speed motions. Moreover, since joint angle errors are not accumulated, high positioning is achieved.[2,3] However, the parallel-link structure still suffers from mass problems of the links because the stiffness of each link must be assured in order to reduce vibration.

In this paper, we propose a new type of parallel robot using wires instead of links. The mass of moving part of the proposed robot is extremely small because the mass of wires can be negligible in comparison with links. Therefore, relatively small motors are able to generate high acceleration and high speed. However, wires can only pull but not push on the object. This case is similar to the problem of multi-fingered grasping, where the fingers can apply only pushing forces on the object. Hence, it is necessary to control the internal forces in the wires, as well as the forces acting on the end effector.

Such parallel wire-driven robots have been already proposed. Higuchi et al. investigated the mechanism of the parallel wire-drive system and showed some experimental results using a two-dimensional robot.[4] Osumi et al. developed a crane to move heavy objects by using the parallel wire mechanism.[5] However, the effect of the parallel wire-drive system on high speed motion has not been made clear. Moreover, it has not been mathematically proven that the position and the orientation of the parallel wire-driven robots converge to desired values.

In this paper, the driving principle of the wire-driven robot is analyzed at first. Next, kinematics and dynamics of the parallel wire-driven robots are described. Then we provide a mathematical proof to guarantee a motion convergence to a desired position and orientation. A Lyapunov function is introduced to prove the motion convergence. Unlike serial link robots, the convergence proof cannot be directly derived from the previous work[6] because of redundant actuation. We point out that the convergence proof is completed by using a result which is obtained from "Vector Closure".[7] In practice, the actuator unit including wire has elasticity which generates vibration in many cases. To reduce vibration, an effective method which uses the internal force among wires is proposed based on analysis with non-linear elasticity. Finally, the effectiveness of the proposed methods in this paper is demonstrated through some experimental results in which a parallel wire-driven robot with seven wires is used.

2. DRIVING PRINCIPLE

2.1. Vector Closure

In this paper, we consider parallel wire-driven robots as shown in Figure 1 (FALCON-7). An object or end-effector

† Department of Robotics, Faculty of Science and Engineering, Ritsumeikan University, Noji-cho, Kusatsu, Shiga, 525-0055 (Japan).
email: kawamura@se.ritsumei.ac.jp
†† Multi-media Center, Shiga University of Medical Science,Seta, Ohtsu, Shiga, 520-2192 (Japan).
email: kino@belle.shiga-med.ac.jp
††† FA Research Institute, Production Engineering Center, SAMSUNG Electronics Co.,Ltd, 416 Maetan3-Dong, Paldal-Gu, Suwon, Gyonggi, 442-742 (Korea).
email: wonchoe@srtf.sec.samsung.co.kr

https://doi.org/10.1017/S0263574799002477 Published online by Cambridge University Press

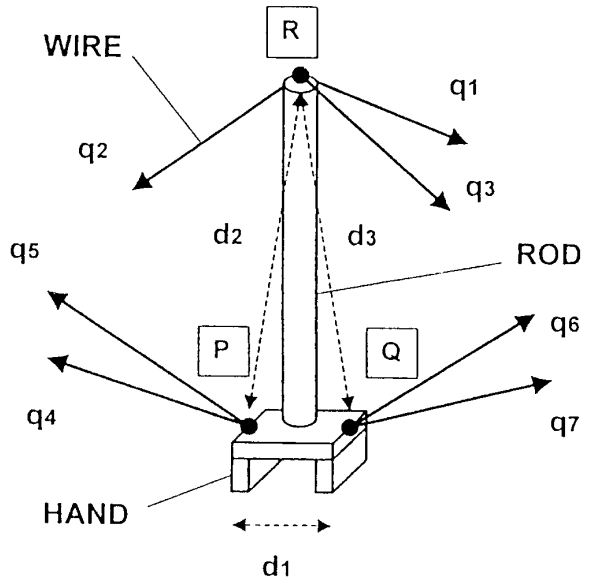

Fig. 1. Structure of a Parallel Wire-Driven Robot (FALCON-7).

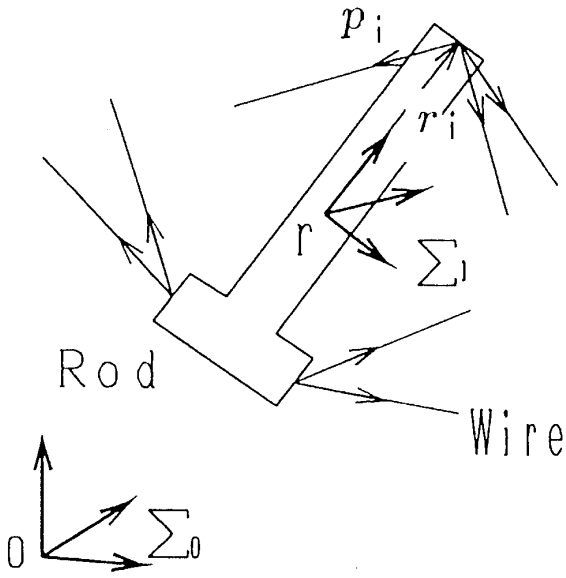

Fig. 2. Definition of Coordinate Systems.

is suspended by wires (tendons). However, since wires can generate only tension, redundant actuation is necessary. This feature is similar to that of multi-finger robots. In fact, the concept "Vector Closure" which was mentioned in the research of multi-finger robots plays a very important role in the research of parallel wire-driven robots.[7] In general, Vector Closure is expressed in the following way:

Vector Closure. *In an n-dimensional space, a set of vector V is a Vector Closure if and only if V has at least n+1 vectors* $(v_1\ v_2\ \ldots\ v_{n+1})$ *satisfying the following two conditions.*

(1) Each set of n vectors in n+1 vectors is linearly independent.
(2) A vector $\beta=(\beta_1\beta_2\ \ldots\ \beta_{n+1})^T$ *exists, which satisfies*

$$V\beta=\sum_{i=1}^{n+1} v_i\beta_i=0 \tag{1}$$

where each element of the vector β *has the same sign (positive or negative), i.e.*

$$\beta_i>0 \text{ (for any } i) \text{ or } \beta_i<0 \text{ (for any } i).$$

Here, let us define wire vectors w_i in order to make clear the relation between Vector Closure and parallel wire driven robots. As shown in Figure 2, the wire vector w_i is given by

$$w_i=\begin{bmatrix} p_i \\ r_i\times p_i \end{bmatrix}, \tag{2}$$

where a vector p_i denotes a directional vector, r_i means a vector between the center of gravity on the object and the connected point of the wire. The mark $\times$ represents a vector product. When the wire tension vector and the resultant force acting on the object are set at $\tau=(\tau_1\tau_2\ \ldots\ \tau_m)^T$ and $f=(f_1f_2\ldots f_n)^T$, respectively, the force relation is expressed by

$$f=W\tau, \tag{3}$$

where the matrix W denotes a wire matrix which is defined by

$$W=[w_1w_2\ \ldots\ w_m]. \tag{4}$$

If we regard the vector w_i and the τ_i as the vector v_i and β_i, the Vector Closure conditions mean that each wire tension remains positive and any resultant force vector can be generated. In other words, the conditions to make a resultant force vector with an arbitrary amplitude and direction are given by those of the Vector Closure. From this result, it is easy to understand that at least n+1 wires are necessary to realize the motion with n degrees of freedom.

2.2. Driving force and internal force

As seen in the previous section, the relation between resultant force f on the object and the wire tension τ is represented by Equation (3). Since the wire number must be larger than that of degrees of freedom, the wire matrix is not square. Therefore, a pseudo-inverse matrix is used to obtain the inverse relation instead of using the usual inverse matrix. The inverse relation to calculate the wire tension from the resultant force is given by

$$\tau=W^+f+(I-W^+W)k_e \tag{5}$$

where the matrix W^+ is a pseudo-inverse matrix of the matrix W. The second term of the right hand side in Equation (5) denotes an internal force among the wires. The internal force does not produce the driving force for the object, but produces tension among the wires. It can be set arbitrary values as the vector k_e is changed.

In previous work with parallel wire-driven robots, the internal force was not utilized effectively. Therefore, it has been considered that the redundancy is a disadvantage of this system. In this paper, however, we will propose a useful method to reduce vibration of the object using such redundant actuation. Since the internal force will play an important role in the proposed method, the calculation of the internal force is explained here. In general, we may determine a vector k_e which makes the second term of the right hand side in Equation (5) positive, because large

https://doi.org/10.1017/S0263574799002477 Published online by Cambridge University Press

positive values of the second term give positive values in the wire tension τ even though the first term is negative. From a theoretical point of view, extremely large values can be set as elements of the vector k_e. In practice, however, the values of the vector k_e are bounded due to saturation of the actuator power. Therefore, we must determine the internal force vector taking account of such actuator saturation. In the case that the wire number is n+1 to realize motion with n degrees of freedom, a convenient way to determine the internal force vector $(I - W^+W)k_e$ is introduced by the Vector Closure. Equation (1) of the Vector Closure condition gives

$$W\tau = \sum_{i=1}^{n+1} w_i \tau_i = 0. \tag{6}$$

Then, we obtain

$$[\tau_1 \tau_2 \ldots \tau_n]^T = -N^{-1} w_{n+1} \tau_{n+1}, \tag{7}$$

where the matrix N denotes $[w_1 w_2 \ldots w_n]$. If the motion area satisfied the conditions of the Vector Closure, each w_i vector is linearly independent. Therefore, non-singularity of the matrix N is guaranteed. Then, we may denote the internal force vector, as follows:

$$\tau = \begin{bmatrix} -N^{-1} w_{n+1} \\ 1 \end{bmatrix} \tau_{n+1}. \tag{8}$$

If we set τ_{n+1} a positive value, all other elements become positive, because the Vector Closure condition is satisfied.

3. KINEMATICS AND DYNAMICS

3.1. Kinematics and inverse kinematics

In this section, kinematics and inverse kinematics are explained. Since each wire length is controlled, we consider the coordinates transformation between wire length coordinates and task-oriented coordinates, such as Cartesian coordinates. Let us consider the coordinates transformation by an example of FALCON-7, as shown in Figure 1. In Figure 1, q_i is the i-th wire length. The ends of three wires are attached to one end of a rod and the ends of the remaining four wires are fixed to the other end of the rod where the robot hand is located; the other end of each wire is connected to the guiding pulley of an actuator unit.

Kinematic calculation is easily obtained in the following manner: At first, we set the points P, Q and R, as seen in Figure 1, and calculate the position of the point R from the following equation:

$$q_i = \| R - A_i \| \ (i = 1, 2, 3) \tag{9}$$

where point A_i denotes a starting point of wire in an actuator unit and " $\| \ \|$ " means Euclidean norm. Next, the points P and Q are determined by

$$d_2 = \| R - P \|, \tag{10}$$

$$q_i = \| P - A_i \| \ (i = 4, 5), \tag{11}$$

$$d_3 = \| R - Q \|, \tag{12}$$

$$q_i = \| Q - A_i | \ (i = 6, 7). \tag{13}$$

Finally, since the positions of the three points P, Q and R are obtained, the position and orientation of the end-effector or hand are calculated. The kinematics from wire length coordinates to the task oriented coordinates has been achieved.

Inverse kinematics is much easier than kinematics. Thus, from the position and the orientation of the end-effector, we obtain the positions of points R, P and Q. By just substituting these values into Equations (9), (11) and (13), the wire lengths are obtained. Generally speaking, kinematics is very difficult in parallel mechanism. However, in a parallel wire mechanism, kinematics is easy because some wires start from the same point.

3.2. Dynamics

We assume that the mass of wire and resistance by the air can be ignored, because they are very much smaller than those of other mechanical parts. Moreover, we suppose that this system satisfies the conditions of a Vector Closure at any time. Under such assumptions, the actuators dynamics is represented by

$$A\ddot{q} + B\dot{q} + \tau = u \tag{14}$$

where,
$q = (q_1, q_2, \ldots, q_7)^T$: wire-length vector,
$\dot{q}$: velocity of vector q,
$\ddot{q}$: acceleration of vector q,
$A = diag.(a_1, a_2, \ldots, a_7)$: actuator inertia matrix (7×7),
$B = diag.(b_1, b_2, \ldots, b_7)$: actuator viscous friction coefficient matrix(7×7),
$\tau = (\tau_1, \tau_2, \ldots, \tau_7)^T$: wire tension vector,
$u = (u_1, u_2, \ldots, u_7)^T$: motor torque vector.

The matrices A and B include the inertia and the viscosity of gears. On the other hand, the rod dynamics is expressed by

$$M\ddot{\phi} + h + d = f \tag{15}$$

where

$$M = \begin{bmatrix} mE_3 & 0 \\ 0 & I \end{bmatrix},$$

m: rod mass,
E_3: unit matrix (3×3),
I: inertia tensor in a base coordinates Σ_0 (3×3),
$h = (0^T, (\omega \times (I\omega))^T)^T$: (6×1)
ω: angular velocity vector (3×1),
$\dot{\phi} = (\dot{r}^T, \omega^T)^T$: (6×1),
$r = (x, y, z)^T$: position of the center of gravity (3×1),
$d = (0, 0, mg, 0, 0, 0)^T$: (6×1),
g: acceleration of gravity (6×1),
f: force and torque vector (6×1).

As seen in Figure 2, the wire tension τ produces the motion of the rod or the robot hand. Hence, the force and torque vector f is given by

$$f = W\tau \tag{16}$$

https://doi.org/10.1017/S0263574799002477 Published online by Cambridge University Press

where $W=[w_1, w_2, \ldots, w_7]$ denotes a wire matrix. In Figure 2, the other coordinates Σ_1 are set at the center of gravity. Therefore, we consider that the position of the center of gravity and the orientation of the coordinates Σ_1 are controlled.

4. CONTROL

4.1. Control in wire length coordinates

Here, we employ a PD feedback control law in the wire length coordinates. Like in parallel link mechanism, inverse kinematics of parallel wire mechanism is easily calculated. As the result, a desired wire length vector q_d, which corresponds to a desired position and an orientation ϕ_d of the task oriented coordinates Σ_0 are obtained. By using the desired vector q_d, the input u is given by

$$u=K_p(q_d-q)-K_v\dot{q}+p+p_g \tag{17}$$

where $K_p(7\times 7)$ and $K_v(7\times 7)$ denote feedback gain matrices. The term $p(7\times 1)$ denotes an internal force vector which satisfies

$$Wp=0. \tag{18}$$

Here, it is important to note that the vector p does not move the rod but causes internal forces. The final term $p_g(7\times 1)$ is added in order to compensate for the gravitational force. The vector p_g must satisfy

$$Wp_g=d. \tag{19}$$

In the following sections, we investigate whether or not the wire length vector q converges to the desired one q_d.

4.2. Property on wire length in Vector Closure space

As regards the stability analysis of the control scheme in wire length coordinates, it cannot be proved that the wire length converges to the desired one by only using the previous Lyapunov method.[6] Therefore, other ideas are needed. Here we will show the important properties of wire lengths in Vector Closure as regards the stability analysis. It assumes that n+1 wires are utilized for n D.O.F.($n\leq 6$), and the system always satisfies the condition of Vector Closure.

It is obvious that the second condition in Vector Closure can be rewritten into

$$-W_1^{-1}w_1=\begin{bmatrix}\eta_1\\ \eta_2\\ \vdots\\ \eta_n\end{bmatrix} \tag{20}$$

$$\eta_i>0 \quad \text{for any i } (1\leq i\leq n)$$

where the matrix $W_1=[w_2 w_3 \ldots w_{n+1}]$ $(n\times n)$.[8] From the first condition in Vector Closure, the matrix W_1 is nonsingular. Here, it is important to note that the element η_i $(1\leq i\leq n)$ is uniquely determined by the wire vectors w_i. Therefore, an arbitrary vector x in null space of the matrix W which satisfies $Wx=0$ leads to the following relation:

$$-W_1^{-1}w_1=[\eta_1\eta_2\ldots\eta_n]^T$$

$$=\left[\frac{x_2}{x_1}\frac{x_3}{x_1}\ldots\frac{x_{n+1}}{x_1}\right]^{\mathrm{T}} \tag{21}$$

where $x=[x_1\ x_2\ \ldots\ x_{n+1}]^T$, if $x_1\neq 0$. The case of $x_1=0$ is included in the trivial solution $x=0$ because of the first condition in Vector Closure. This means that each element of an arbitrary vector x has the same sign. Hence, we obtain the following result:

> RESULT 1
> *If $n+1$ vectors $w_i(1\leq i\leq n+1)$ in a n-dimensional space are Vector Closure, vectors $x=[x_1\ x_2\ \ldots\ x_{n+1}]^T$ which belong to the null space of the matrix $W=[w_1 w_2\ \ldots\ w_{n+1}]$ are given by*
>
> *CASE(1) $x_i=0$ for any i,*
> *or*
> *CASE(2) $x_i>0$ for any i,*
> *or*
> *CASE(3) $x_i<0$ for any i.*

On the other hand, from the Principle of Virtual Work, we obtain

$$\delta q=W^T\delta\phi \tag{22}$$

where δq and $\delta\phi$ denote minute changes of the wire length coordinates and task-oriented coordinates.

The vector β which is given by the Vector Closure condition yields

$$\beta^T\delta q=\beta^T W^T\delta\phi=0 \tag{23}$$

because $W\beta=0$. By integrating Equation (23), we have

$$\sum_{i=0}^{n+1}\int_{q_{is}}^{q_{ie}}\beta_i(q)dq_i=0 \tag{24}$$

where q_{is} and q_{ie} denote start position and end position of each element respectively. Here, it is important to note that each element of the vector β changes depending on q but keeps the same sign (positive or negative) as long as it satisfies the Vector Closure conditions. Hence, it is concluded that the vector q_e-q_s $(q_e=(q_{1e}\ldots q_{n+1e})^T$, $q_s=(q_{1s}\ldots q_{n+1s})^T)$ must contain both positive elements and negative elements in order to satisfy Equation (24). In other words, we obtain the following result.

> RESULT 2
> *If two vectors q_e and q_s are in a Vector Closure space, the difference vector q_e-q_s must contain both positive and negative elements.*

4.3. Stability proof

Now, we are in a position to prove the stability of parallel wire-drive robots. Consider a Lyapunov function, which is similar to Arimoto's Lyapunov function[6] as follows:

https://doi.org/10.1017/S0263574799002477 Published online by Cambridge University Press

$$V=\frac{1}{2}\dot{q}^T A\dot{q}+\frac{1}{2}\dot{\phi}^T M\dot{\phi}$$

$$+\frac{1}{2}(q_d-q)^T K_p(q_d-q). \quad (25)$$

The time derivation of the Lyapunov function V is given by

$$\dot{V}=\dot{q}^T A\ddot{q}+\dot{\phi}^T M\ddot{\phi}$$

$$+\frac{1}{2}\dot{\phi}^T\dot{M}\dot{\phi}-\dot{q}^T K_p(q_d-q). \quad (26)$$

By substituting Equations (14) and (15), we obtain

$$\dot{V}=\dot{q}^T(-B\dot{q}-\tau+u)+\dot{\phi}^T(-h-d+f)$$

$$+\frac{1}{2}\dot{\phi}^T\dot{M}\dot{\phi}-\dot{q}^T K_p(q_d-q).$$

Moreover, from Equations (16) and (17) the above equation can be rewritten into

$$\dot{V}=\dot{q}^T(-B\dot{q}-\tau+K_p(q_d-q)-K_v\dot{q}+p+p_g)$$
$$+\dot{\phi}^T(-h-d+W\tau) \quad (27)$$
$$+\frac{1}{2}\dot{\phi}^T\dot{M}\dot{\phi}-\dot{q}^T K_p(q_d-q).$$

Here we utilize the relation between $\dot{q}$ *and* $\dot{\phi}$, and non-linear characteristic as follows:

$$\dot{q}=W^T\dot{\phi}, \quad (28)$$

$$\dot{\phi}^T(\frac{1}{2}\dot{M}\dot{\phi}-h)=0. \quad (29)$$

From Equations (18), (19), (28) and (29), we obtain

$$\dot{V}=-\dot{q}^T(B+K_v)\dot{q}\leq 0. \quad (30)$$

Finally, we know that the motion converges to a maximum invariant set which satisfies $\dot{V}=0$. In this case, since $\dot{V}=0$ means $\dot{q}=0$, from Equation (28) we have $\dot{\phi}=0$. Therefore, from Equations (14)~(19), the maximum invariant set denotes

$$WK_p(q_d-q)=0. \quad (31)$$

In general, the vector $K_p(q_d-q)$ can have both a trivial solution $(K_p(q_d-q)=0)$ and a non-trivial solution $(K_p(q_d-q)\neq 0)$, because of the non-square matrix W. In the case of a non-trivial solution, the motion stops at some point q_0 which is not equal to the desired point q_d. However, from Result 1 and Result 2 we easily understand that the non-trivial solution cannot exist. Hence, we conclude

$$q=q_d \quad (32)$$

as time t tends to infinity as long as the motion is within the Vector Closure space. Moreover, from Equation (17) we know

$$u=p+p_g, \quad (33)$$

as time tends to infinity.

4.4. Constant gravitational compensation

In the proposed control law, it may be too difficult to calculate the gravitational compensation p_g in real-time. Instead of a real-time calculation for gravitational compensation, a constant value which balances at the desired point is useful. In this case, the input vector is given by

$$u=K_p(q_d-q)-K_v\dot{q}+p+p_{gd}, \quad (34)$$

where the vector $p_{gd}(7\times 1)$ is constant gravitational compensation which balances at the desired point. we obtain the p_{gd} *as*

$$p_{gd}=\frac{\partial\phi}{\partial q}\Big|_{q_d}^T d \quad (35)$$

Considering another scalar function V^*.

$$V^*=\frac{1}{2}\dot{q}^T A\dot{q}+\frac{1}{2}\dot{\phi}^T M\dot{\phi}+\frac{1}{2}(q_d-q)^T K_p(q_d-q)+Q \quad (36)$$

where

$$Q=U(q)-U(q_d)-p_{gd}^T(q-q_d), \quad (37)$$

$U(q)$ denotes the potential energy with the wire length vector q. Moreover, note that Taylor's expansion of $U(q)$ can be expressed as

$$U(q)=U(q_d)+\frac{\partial U}{\partial q}\Big|_{q_d}(q-q_d)+T, \quad (38)$$

where the third term T of the right hand is assumed to be the term greater than a square term. Now, we pay attention to be the following relation:

$$\frac{\partial U}{\partial q}\Big|_{q_d}^T=(\frac{\partial U\partial\phi}{\partial\phi\partial q}\Big|_{q_d})^T=\frac{\partial\phi}{\partial q}\Big|_{q_d}^T d=p_{gd}. \quad (39)$$

At last, from Equations (38) and (39) we know that $Q=T$. Therefore, if eigenvalues of K_p are sufficiently large, V^* can become a part of a Lyapunov function. The time derivation of V^* is obtained in the exactly same manner in Equation (30). Then motion convergence is guaranteed by the same treatment from Equation (31) and Equation (32).

5. STIFFNESS OF PARALLEL WIRE DRIVEN ROBOTS

5.1. Actuator unit

In the parallel wire systems, each wire is rolled by a pulley which is driven by a motor with gears. One example of the actuator unit which will be used in experiments with a high-speed robot is shown in Figure 3. The D.C. servo motor has 60 W capacity and a rotary encoder with resolution 1000 p/rev. The pulley and the gears are made of hard plastic because the total inertia of the system should be small in order to realize high acceleration. The pulley diameter is 65 mm and the gear ratio is 1:3. The guiding pulley is set to let each wire follow the direction of the end-effector.

https://doi.org/10.1017/S0263574799002477 Published online by Cambridge University Press

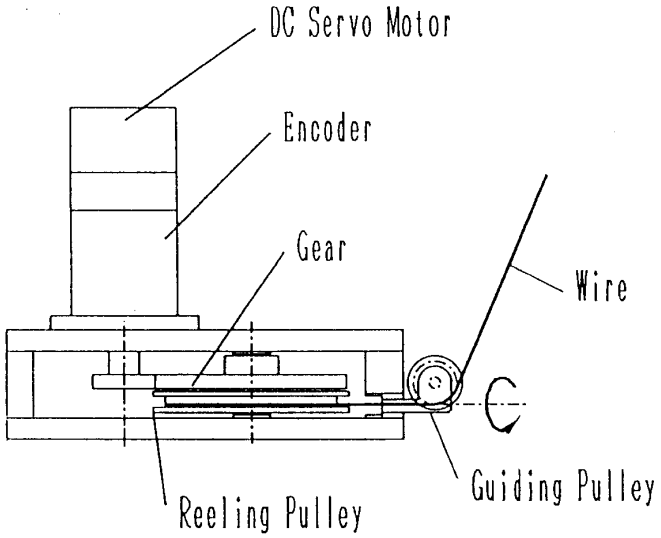

Fig. 3. An actuator.

Generally speaking, wires contain some elasticity, and mechanical parts such as pulleys and gears also have elasticity. It is natural to consider that the elasticity will cause vibration in the motion control of robots. To find a solution of the problem, we investigate the detail feature of elasticity of wire-driven systems in the following section.

5.2. Nonlinear elasticity of parallel wire-driven robot

Of course, the elasticity of the wire itself was much investigated in the research of wires. In the parallel wire-driven robot systems, however, total elasticity including pulleys and gears must be measured in order to consider the vibration problem. The experimental system shown in Figure 4 is used in order to measure the total elasticity. In the measurement system, the actuator unit for high speed robots explained in the previous section is utilized, and we set wire length at 1 m. The gear of motor side is mechanically locked. The load for the wire and mechanical parts is increased by adding the weights. The displacement of the weights is measured by a laser sensor with a 50 micro-m resolution . The measurement result is shown in Figure 5. As seen in Figure 5, there is hysteresis. If it is assumed that the parallel wire-driven robot can move and preserve the desired internal forces, we may consider only loading-up path of the hysteresis in Figure 5. Even though we restrict the loading-up path, it still contains non-linearity. To represent the non-linearity of elasticity, we introduce the following relation between displacement x and force (load) f:

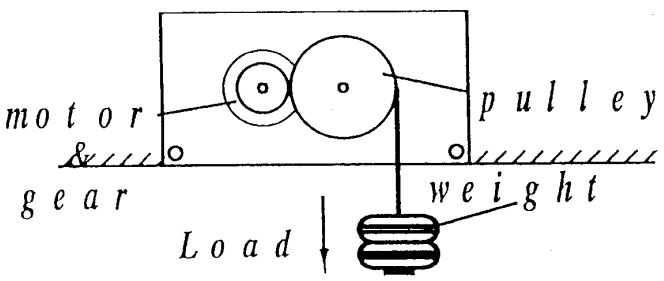

Fig. 4. Experimental System.

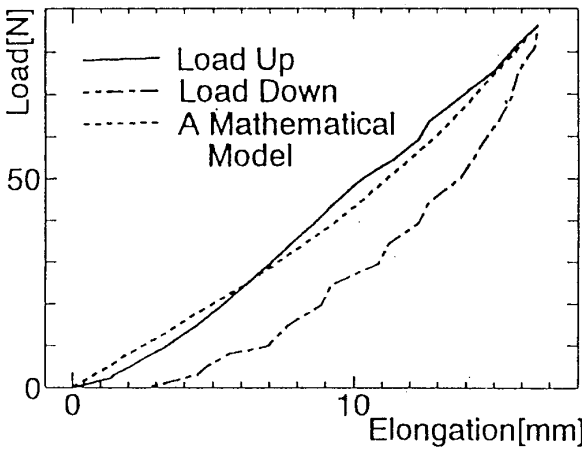

Fig. 5. Elasticity of a Wire-Driven System.

$$f = k_1 x + k_2 x^3. \tag{40}$$

In the above model, the parameters k_1 and k_2 were estimated at $k_1 = 3.8 \times 10^3$ *N/m* and $k_2 = 5.0 \times 10^6$ *N/m*^{3}, respectively.

5.3. Internal force stiffness

In this section, we investigate how the non-linear elasticity influences the total system of parallel wire-driven robots. At first, let us consider a simple example as seen in Figure 6. There two wires with non-linear elasticity including mechanical parts are set and both wire have same coefficients k_1 and k_2. Since the original wire length is l_0 and the equilibrium state causes a wire length l_1, the center point is balanced with an internal force f_{int} given by

$$f_{int} = k_1(l_1 - l_0) + k_2(l_1 - l_0)^3. \tag{41}$$

Here, it is easy to calculate the stiffness on the center point (x = 0, y = 0, z = 0) in the following way:

$$K_x = \left.\frac{\partial f_x}{\partial x}\right|_{x=y=z=0} = 2k_1 + 6k_2(l_1 - l_0)^2, \tag{42}$$

$$K_y = \left.\frac{\partial f_y}{\partial y}\right|_{x=y=z=0} = 2k_1\frac{l_1 - l_0}{l_1} + 2k_2\frac{(l_1 - l_0)^3}{l_1}, \tag{43}$$

$$K_z = \left.\frac{\partial f_z}{\partial z}\right|_{x=y=z=0} = 2k_1\frac{l_1 - l_0}{l_1} + 2k_2\frac{(l_1 - l_0)^3}{l_1}, \tag{44}$$

where f_x, f_y, f_z are forces in x-, y-, z-directions, and K_x, K_y, K_z are stiffness coefficients in x-, y- and z-directions.

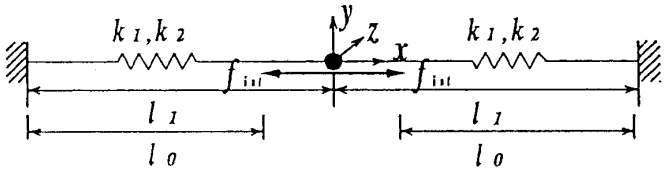

Fig. 6. 1 D.O.F. Wire-Driven System Model.

https://doi.org/10.1017/S0263574799002477 Published online by Cambridge University Press

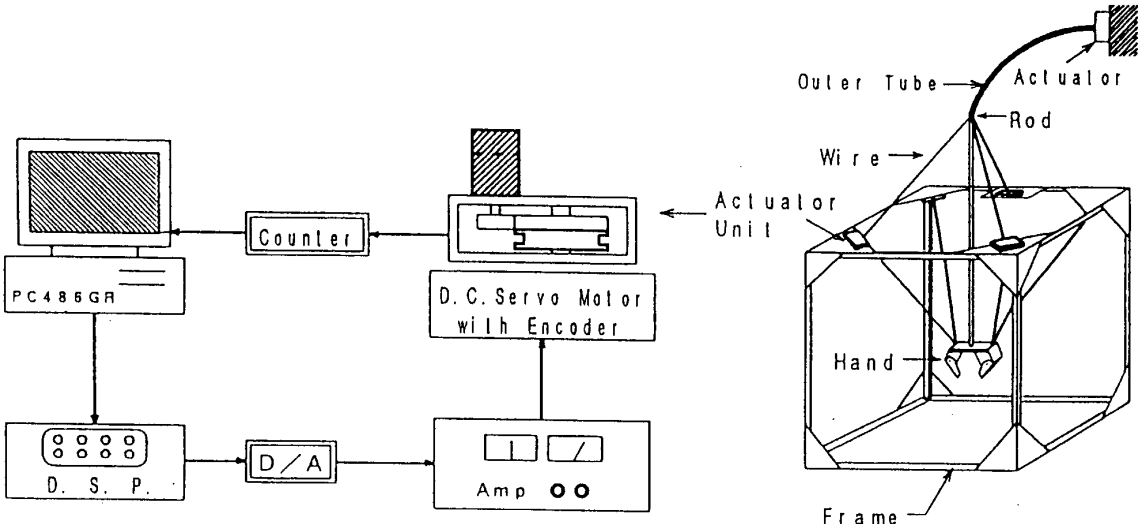

Fig. 7. High Speed Robot FALCON-7.

In the above equations, it is understood that the stiffness of the center point for all direction (x-, y- and z-directions) increases as the internal force f_{int} becomes large. Moreover, it should be noted that the stiffness in the x-direction is much larger than those of y- and z- directions because the difference $l_1 - l_o$ is 10^{-2} m in the case that the wire lengh l_1 is about 1 m. Now, we summarize the internal force stiffness. As seen in Equations (42), (43) and (44), the internal force stiffness is divided into two classes as follows:

- *internal force stiffness in the direction of the wire tension (x-direction in Figure 6).*

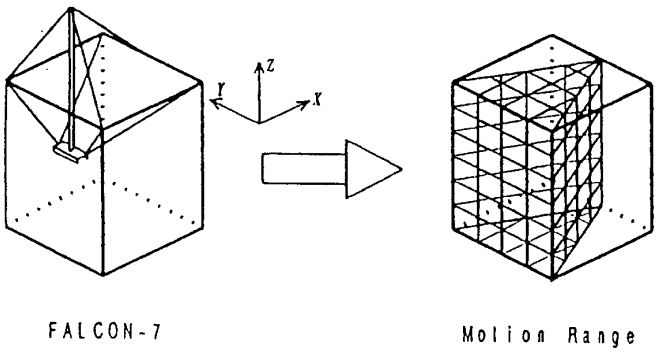

Fig. 8. Translational Range of FALCON-7.

Table I. Rotational Range of FALCON-7

Position (x,y,z)	x-axis [deg]	y-axis [deg]	z-axis [deg]
(500, 500, −500)	±25	±45	±45
(500, 500, −700)	±19	±33	±45
(500, 500, −300)	±35	±59	±45
(500, 700, −500)	+41 ~ −4	+9 ~ −45	±35
(500, 300, −500)	+4 ~ −41	+9 ~ −45	±35
(700, 500, −500)	±15	+30 ~ −53	±30
(300, 500, −500)	±33	+53 ~ −30	±30

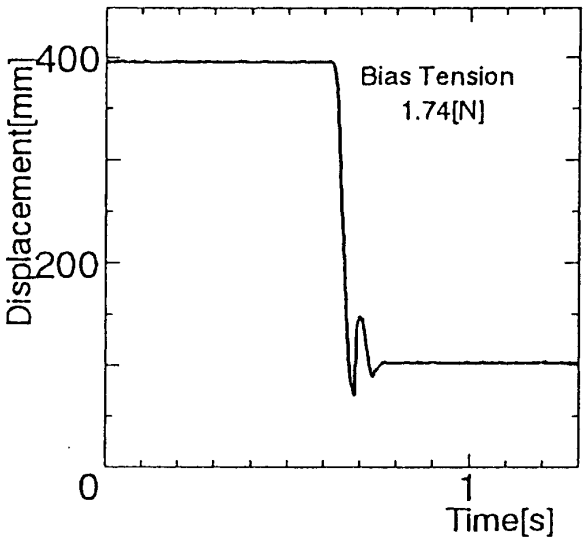

Fig. 9. Step Response (Low Internal Force).

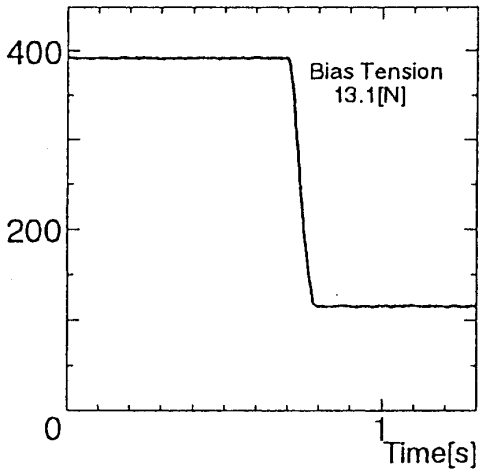

Fig. 10. Step Response (High Internal Force).

https://doi.org/10.1017/S0263574799002477 Published online by Cambridge University Press

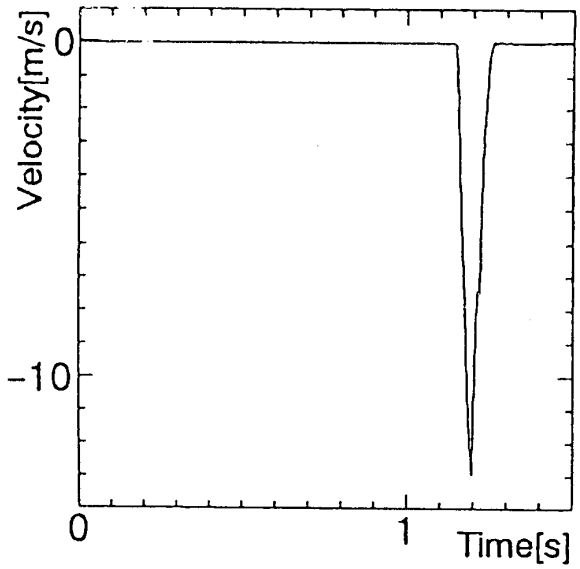

Fig. 11. Velocity Signal.

- *internal force stiffness in the perpendicular direction of the wire tension (y- and z-directions in Figure 6).*

About the two kinds of stiffness, it is important to note the following facts.

(i) As explained in the simple case with two wires, the former is dominant in the parallel wire-driven systems.

(ii) If the parameter k_2 is equal to zero, the former does not occur or linear springs cannot cause internal stiffness in the direction of the wire tension. Even though the parameter k_2 is set to zero, the later exists.[9] Therefore, the internal force stiffness increases as the internal force becomes large in both linear and non-linear springs.

From the above results, we understand that the internal force stiffness in the direction of the wire tension should be effectively utilized to design parallel wire-driven robots. Moreover, it is noted that even if the value from the internal force stiffness of the perpendicular direction of the wire tension is small, it causes an increase of the total stiffness.

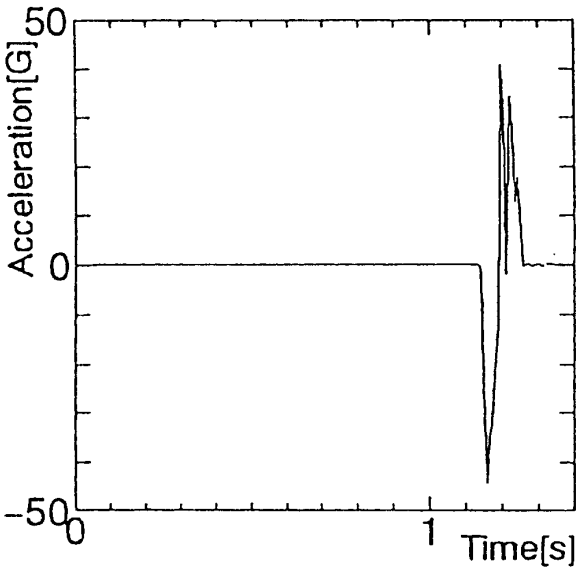

Fig. 12. Acceleration Signal.

6. EXPERIMENTAL RESULTS

6.1. High speed robot FALCON-7

A high speed robot FALCON-7(Fast Load Conveyance robot with 7 wires) is designed. The schematic configuration of the FALCON-7 ultra-high speed manipulator is shown in Figure 7. This system utilizes seven wires to achieve motion with six degrees of freedom. The gripper is moved by another motor via one wire which goes inside of the rod. The dimensions of the manipulator frame are 1.45 m × 1.45 m × 1.25 m. The wires are made of steel 0.54 mm diameter. The rod is made of duralumin, and has a length of 1 m and a mass of 150 g. Another advantage of the proposed configuration is that a larger motion range can be obtained using the same motor and pulley, if longer wires are used.

A translational motion range with fixed orientations of the rod is shown in Figure 8. Table I lists the rotational range for specified (x, y, z) positions. If a cubic motion range is needed, we may use four wires to move the top of the rod.

6.2. Experimental results

At first, internal forces at a start point and a desired point are calculated through Equation (7). Next, constant gravitational compensation vectors at the start point and the desired point are obtained by Equation (35). The desired wire length for each wire is determined based on the inverse kinematics given by Equations (9)~(13). We used the control input represented by Equation (17)

Now we show some experimental results utilizing the PD feedback control law in wire length coordinates with a constant gravitational compensation. For a representative case, Figure 9 shows the z-directional motion under a low internal force. In this case, the transient response of the system is quite oscillatory. When the internal force is increased, Figure 10 shows that the overshoot is eliminated completely.

As shown in Figure 11 and Figure 12, the manipulator attains a peak speed of about 13 m/s, and a peak acceleration of 43 g. In this case, the rod is moved in the z-direction over a distance of 0.325 m in a time interval of 0.08 s.

7. CONCLUSION

In this paper, we have proposed a high speed robot by using a parallel wire-driven mechanism. The driving principle, kinematics and dynamics of the parallel wire-driven robot are described. Motion convergence using PD feedback control in wire length coordinates has been proven with a Lyapunov function and Vector Closure. Non-linear elasticity of the parallel wire-driven robot has been investigated and a method to reduce vibration has been proposed. By the experimental results, it has been shown that ultra-high speed

https://doi.org/10.1017/S0263574799002477 Published online by Cambridge University Press

with more than 40 g(g:gravitational acceleration) and peak velocities of 13 *m/s* can be attained without vibration, even though relatively small D.C. motors are used.

References

1. S.H. Li, N. Fujiwara and H. Asada, "An Ultrahigh Speed Assembly Robot System: Part 1. Design", *Proc. IEEE Japan-USA Symp. P. Flexible Automation* (1994) pp. 465–472.
2. R. Clavel, "DELTA, a fast robot with parallel geometry", *Proc. International Symposium on Industrial Robots* (1988) pp. 91–100.
3. F. Pierrot and P. Dauchez et al. "HEXA, a fast six-DOF-fully parallel robot", *Proc. the 5th International Conference on Advanced Robotics '91 ICAR* (1991) pp. 1158–1163.
4. T. Higuchi and A. Ming: "Study on Multiple Degree-of-Freedom Positive Mechanism Using Wires", *Proceeding of Asian Conference on Robotics and its Application* (1991) pp. 101–106.
5. H. Osumi, Y. Shen and T. Arai, "The Manipulability of Wire Suspension System" Trans. Robotics Society of Japan **12**, No.7 1049–1055 (in Japanese) 1994.
6. S. Arimoto, "Control Theory of Non-linear Mechanical Systems" (Clarendon Press, Oxford, 1996).
7. V.D. Nguyen, "Constructing Force-Closure Grasp in 3D", *Proc. of the 1987 IEEE Int. Conf. on Robotics and Automation* (1987) pp. 240–245.
8. S. Kawamura and K. Ito, "A New Type of Master Robot for Teleoperation Using A Radial Wire Drive System" *Proc. of the 1993 IEEE/RSJ Int. Conf. on Intelligent Robots and Systems* (1993) **Vol. 1**, pp. 55–60.
9. M.A. Adli, K. Nagai, K. Miyata and H. Hanafusa, "Analysis of Internal Force Effect in Parallel Manipulators", *Trans. Society of Instrument and Control Engineers* **27** 27–34 (1991).

https://doi.org/10.1017/S0263574799002477 Published online by Cambridge University Press